Journal of Physics: Condensed Matter

PAPER

Superconductivity in the Einstein solid V $Al_{10.1}$

J. Phys.: Condens. Matter **24** (2012) 365701 (4pp) doi:10.1088/0953-8984/24/36/365701

Superconductivity in the Einstein solid $VAl_{10.1}$

T Klimczuk[1,2], M Szlawska[3], D Kaczorowski[3], J R O'Brien[4] and D J Safarik[5]

[1] European Commission, Joint Research Center, Institute for Transuranium Elements, Postfach 2340, D-76125 Karlsruhe, Germany
[2] Faculty of Applied Physics and Mathematics, Gdansk University of Technology, Narutowicza 11/12, 80-952 Gdansk, Poland
[3] Institute of Low Temperature and Structure Research, Polish Academy of Sciences, P Nr 1410, PL-50-590 Wrocław 2, Poland
[4] Quantum Design, 6325 Lusk Boulevard, San Diego, CA 92121, USA
[5] Los Alamos National Laboratory, Los Alamos, NM 87545, USA

E-mail: tomasz.klimczuk@ec.europa.eu

Received 9 June 2012, in final form 24 July 2012
Published 15 August 2012
Online at stacks.iop.org/JPhysCM/24/365701

Abstract
We used magnetic susceptibility, resistivity and heat capacity measurements to characterize the superconducting state in the Einstein solid $VAl_{10.1}$. We find that $VAl_{10.1}$ is a weak-coupling, type-II superconductor with $T_c = 1.53$ K and an upper critical field of $H_{c2}(0) = 800$ Oe. The heat capacity data in the range 0.07 K $< T <$ 1.53 K are consistent with an isotropic energy gap of $\Delta_0 = 0.23$ meV.

(Some figures may appear in colour only in the online journal)

'Rattling' refers to the low frequency and sometimes anharmonic vibrations of guest atoms that occupy oversized polyhedral cages. Several crystal families are known to contain rattling modes, including clathrates [1–4], skutterudites [5], β-pyrochlores [6] and dodecaborides [7]. In most cases the rattling coexists with other interesting behavior, such as strong scattering of acoustic phonons [1, 2] and superconductivity [6]. The phonon scattering is currently understood in terms of avoided crossings of the rattling mode optical branches with host-lattice acoustic branches [8].

For superconductivity the role of rattling is less clear. Nagao *et al* [6] showed that for the β-pyrochlore oxides AOs_2O_6 (A = Cs, Rb, K) the character of the superconductivity changes systematically from weak coupling for the Cs^+ guest ($T_c = 3.25$ K), which has the largest size and highest vibrational frequency, to strong coupling for K^+ ($T_c = 9.6$ K), which has the smallest size and lowest frequency. Based on their strong-coupling analysis, Nagao *et al* [6] concluded that the rattling modes of the these ions dominate the electron–phonon interaction function and thus mediate the formation of Cooper pairs. NMR studies of the K sites in KOs_2O_6 also point to strong coupling of the rattling phonons to the electrons [9]. At least for the β-pyrochlore oxides, it appears that superconductivity is enhanced by a small guest atom having low rattling frequency and large dynamic displacements from the cage center. Large displacements are particularly favored when the rattling has strong anharmonicity even in the ground state.

For the dodecaborides ZrB_{12} and LuB_{12} [7], replacement of the Zr guest with the larger Lu guest reduces T_c from 6.0 to 0.4 K. This reduction is accompanied by a change from strong- to weak-coupling, and by a much reduced role of the rattling in the electron–phonon interaction. Surprisingly, though, the rattling frequency is largely unaffected by the substitution of Lu for Zr. Given that these guests have such different positions in the periodic table, we cannot easily distinguish chemical effects from those of the rattling itself, as was possible in the pyrochlores. Based on the available literature data, it is fair to say that at present we do not understand which characteristics of rattling are relevant to superconductivity.

Rattling modes in VAl_{10} were first reported in the early 1970s. Large anomalies in the low-temperature heat capacity, electrical resistivity, and thermal expansion were explained by

assuming that VAl_{10} contains a large density of optical phonon modes, all with an Einstein temperature of $\theta_E \approx 22$ K [10, 11]. The dominance of these low-energy dispersionless modes was considered so unusual that Caplin *et al* called VAl_{10} an Einstein solid [10]. Inductance measurements later showed that VAl_{10} superconducts below 1.6–1.7 K [12], but the role of Al impurities in the observed behavior was not clear. Our recent heat capacity measurements confirmed bulk superconductivity in $VAl_{10.1}$ [13]. We also showed that the Al guests in $VAl_{10.1}$ rattle with strong anharmonicity, having a frequency that increases with amplitude akin to a particle in a box. Considering the strong anharmonicity and low frequency, we are motivated to investigate the possible role of rattling in the superconductivity of $VAl_{10.1}$. To this end, in the present work we characterize the superconducting properties of $VAl_{10.1}$.

Polycrystalline samples of $VAl_{10.1}$ were synthesized by arc-melting Al and V in a high-purity Ar atmosphere. More details on the synthesis procedure are given in [13]. The magnetization was measured in a commercial superconducting quantum interference device (SQUID) magnetometer from Quantum Design, equipped with a ^{3}He refrigerator. Measurements were done in the range 0.4 K $\leq T \leq$ 1.8 K at fields of up to 800 Oe. Electrical resistivity and heat capacity were measured using Quantum Design Physical Properties Measurement Systems equipped with ^{3}He and dilution refrigerators. Resistivity measurements were performed in the range 0.4 K $\leq T \leq$ 300 K at fields of up to 2300 Oe. We used a four-probe AC technique with copper wires spot-welded to the specimens employing a home-built welder and welding conditions (pressure, current, and operation time) adjusted by trial-and-error method. Heat capacity was measured in the range 0.07 K $\leq T \leq$ 300 K at fields of up to 1000 Oe using a thermal relaxation technique.

Previous neutron and x-ray diffraction measurements [13] verified that our $VAl_{10.1}$ samples contained mainly the $VAl_{10+\delta}$ phase, with cubic $Mg_3Cr_2Al_{18}$-type structure. The crystal structure is discussed in [13, 14]. From Rietveld refinements we determined $a = 14.5143(5)$ Å at 300 K. This is larger than the room-temperature value of 14.492(4) Å reported for VAl_{10} [14], and close to 14.516 Å reported for V_4Al_{41} [15]. Our samples contained an Al impurity with concentration <5 wt% as determined from the refinements. Based on these data and the nominal composition $VAl_{10.1}$, we estimate that the $VAl_{10+\delta}$ phase has composition $\delta \approx 0.05$–0.1. This corresponds to 10–20% occupancy of the cage site with rattling Al atoms. We attempted to prepare alloys with higher occupancy, but the extra Al created more impurity phase rather than filling the cages.

Figure 1(a) shows the temperature dependence of the zero-field-cooled magnetic susceptibility normalized to $1/4\pi$, and measured in fields from 20 to 600 Oe. For the 20 Oe applied field (the lowest that we measured) the transition temperature is 1.5 K. Here we define the transition temperature as the point where the extrapolation of the steepest slope of the $\chi_V(T)$ data intersects the extrapolation of the normal-state data [16]. This is shown in figure 1(a). The

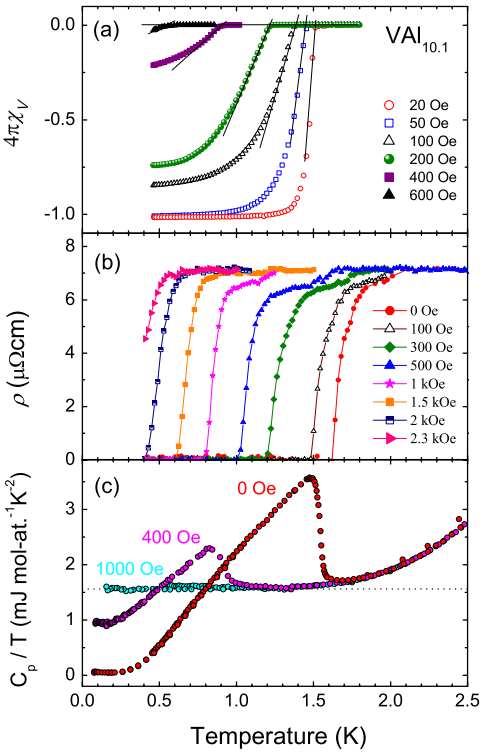

Figure 1. Temperature dependences of: (a) the zero-field-cooled magnetic susceptibility; (b) the electrical resistivity; (c) the specific heat C_p/T. All measurements were performed under zero field and for the indicated applied magnetic fields. The horizontal dashed line in the inset (c) corresponds to $\gamma = 1.56$ mJ mol atoms^{-1} K^{-1}.

superconducting transition is sharp, and there is no evidence of another transition at 1.175 K that would be associated with pure Al metal.

Figure 1(b) shows the temperature dependence of the electrical resistivity near the superconducting transition, measured for applied magnetic fields between 0 to 2.3 kOe. A double transition is observed for fields below 1 kOe. Even for 2.3 kOe, which is almost three times as large as the $H_{c2}(0)$ estimated from the magnetic and the heat capacity measurements (see figure 2), we still observe the superconducting transition. The discrepancy in comparing the magnetic and heat capacity data to the resistivity measurements is likely caused by the Al impurity in our samples. Pure Al in the form of a granular film can superconduct at T_c up to 2.9 K and with H_{c2} exceeding 10 kOe [17].

The temperature dependence of the heat capacity, plotted as C_p/T versus T, near the superconducting transition is shown in figure 1(c). Data are displayed for 0, 400, and 1000 Oe. The large jump at $T_c = 1.53$ K in the zero-field data confirms the bulk nature of superconductivity. In a field of 1 kOe, C_p/T is featureless to 100 mK. This is consistent with $H_{c2}(0) \approx 800$ Oe determined from our magnetic measurements.

Figure 2 shows the temperature dependence of the upper critical field H_{c2}, as determined from the magnetic susceptibility measurements and from the heat capacity data. Assuming that $VAl_{10.1}$ is a dirty type-II superconductor,

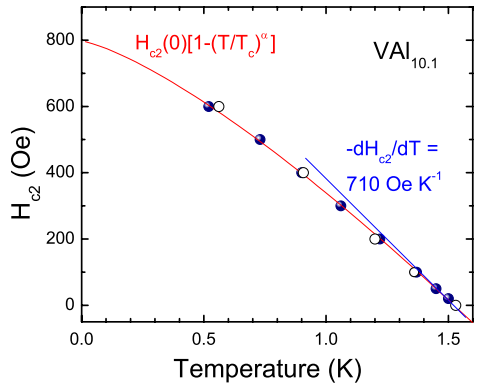

Figure 2. The upper critical field H_{c2} as a function of temperature, determined from the magnetic susceptibility data (closed symbols) and from the heat capacity data (open symbols). The fitting lines are described in text.

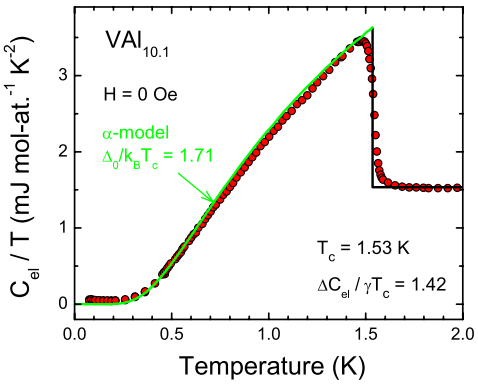

Figure 3. Temperature dependence of the electronic heat capacity, plotted as C_{el}/T. The curve through the data shows the fit of the α-model for $\Delta_0/k_BT_c = 1.71$.

we estimate the upper critical field at 0 K using the Werthamer–Helfand–Hohenberg (WHH) equation [18], $H_{c2}(0) = -0.693(dH_{c2}/dT)_{T=T_c}T_c$. Approximating the zero-field critical temperature as $T_c(0) \approx T_c(20\ \text{Oe}) = 1.5$ K and using the initial slope $dH_{c2}/dT = -710$ Oe K^{-1} through the lowest-field points, we calculate $H_{c2}(0) = 740$ Oe. We have also estimated $H_{c2}(0)$ by fitting all of our $H_{c2}(T)$ data using the empirical power law expression $H_{c2} = H_{c2}(0)(1 - (T/T_c)^{\alpha})$. This fit is shown in figure 2 by the curve through data. From the fit we estimate $H_{c2}(0) = 800(90)$ Oe, $T_c = 1.52(1)$ K, and $\alpha = 1.32(5)$. If we assume that the upper critical field originates only from orbital effects, the coherence length can be estimated using the Ginzburg–Landau formula $\xi_{GL}(0) = (\phi_o/2\pi H_{c2}(0))^{1/2}$, where ϕ_o is the quantum flux. Using the value $H_{c2}(0) = 800$ Oe, we estimate $\xi_{GL}(0) = 64$ nm.

Recently we analyzed the normal-state specific heat of $VAl_{10.1}$, focusing on the rattling of the Al guest atoms [13]. In this analysis we assumed that besides the usual γT electronic and βT^3 phonon contributions at low temperature, there is an additional contribution from the rattling of the Al guests. We found that this contribution is best described in terms of a sixth-order interatomic potential [13]. From our analysis we deduced a characteristic temperature of $\theta_{RM,6} = 21$ K for the rattling. We also determined a Debye temperature of $\theta_D = 341$ K and a Sommerfeld coefficient of $\gamma = 1.56$ mJ mol-at.$^{-1}$ K^{-2} (17.3 mJ mol^{-1} K^{-2}). Based on this analysis, in [13] we estimated the phonon contribution to the low-temperature heat capacity. Figure 3 shows the temperature dependence of the electronic heat capacity C_{el}/T, determined by subtracting this phonon contribution from the measured data. An equal-entropy analysis gives $T_c = 1.53$ K and $\Delta C_{el}/\gamma T_c = 1.42$. The former value agrees with the T_c determined from our magnetic measurements, while the latter is close to 1.43, which is the value predicted by the BCS theory for weak coupling [19].

Using the inverted McMillan's formula [20],

$$\lambda_{ep} = \frac{1.04 + \mu^* \ln(\frac{\theta_D}{1.45T_c})}{(1 - 0.62\mu^*)\ln(\frac{\theta_D}{1.45T_c}) - 1.04}, \qquad (1)$$

we can estimate the electron–phonon coupling constant λ_{ep}. Assuming values of $\mu^* = 0.1$ and 0.15 for the Coulomb repulsion constant we calculate $\lambda_{ep} = 0.42$ and 0.51, respectively. This again suggests that $VAl_{10.1}$ is a weak-coupling superconductor. From these values of λ_{ep} and $\gamma = 17.3$ mJ mol^{-1} K^{-2} we calculate the electronic density of states at the Fermi energy for both spin directions. We find $N(E_F) = 3\gamma/[\pi^2 k_B^2(1 + \lambda_{ep})] = 5.2$ and 4.9 states eV^{-1} per formula unit for $\lambda_{ep} = 0.42$ and 0.51, respectively. Previously [13] we used the thermal conductivity and electrical resistivity data to estimate a normal-state quasiparticle mean free path of $l_0 = 2$–4 nm for $T < 10$ K. Together with our present estimate of $\xi_{GL}(0) = 64$ nm, we find that $\xi_{GL}(0)/l_0 = 16$–32. This confirms our earlier assumption that $VAl_{10.1}$ is in the dirty limit.

Using our heat capacity data for the normal and superconducting states, $C_p(1\ \text{kOe})$ and $C_p(0\ \text{Oe})$, we now calculate the thermodynamic critical field $\mu_0 H_c^2(0)/2 = \int\int (C_p(1\ \text{kOe})/T - C_p(0\ \text{Oe})/T)\,dT$. We obtain a zero-Kelvin critical field of $H_c(0) = 148$ Oe. The relationship between the upper, lower, and thermodynamic critical fields is $H_{c1}H_{c2} = H_c^2 \ln\kappa$, where $\kappa = \lambda_{GL}/\xi_{GL}$ is the Ginzburg–Landau parameter and λ_{GL} is the penetration depth. If we substitute into this equation the expressions for the upper and lower critical fields, $H_{c1} = \phi_0 \ln\kappa/4\pi\lambda_{GL}^2$ and $H_{c2} = \phi_0/2\pi\xi_{GL}^2$, and solve for the penetration depth we find $\lambda_{GL} = \phi_0/2\sqrt{2}\pi\ H_c\xi_{GL}$. Using the coherence length estimated earlier, $\xi_{GL} = 64$ nm, together with $H_c(0) = 148$ Oe we estimate $\lambda_{GL} = 245$ nm. From this value of the penetration depth we compute $\kappa = \lambda_{GL}/\xi_{GL} = 3.8$. This verifies that $VAl_{10.1}$ is a type-II superconductor, as we have assumed throughout this analysis. Finally, from the values of $H_c(0)$ and κ, together with $H_{c2}(0) = 800$ Oe, we estimate a lower critical field of $H_{c1}(0) = 37$ Oe. Table 1 summarizes superconducting parameters and other physical properties of $VAl_{10.1}$.

The curve through the data in figure 3 shows the temperature dependence of C_{el}/T for the range $0 < T \leq T_c$ as predicted by the α-model semiempirical modification of BCS theory [21]. In the α-model the gap ratio Δ_0/k_BT_c is an adjustable parameter, but the temperature dependence

Table 1. Physical properties and superconducting parameters for $VAl_{10.1}$.

T_c (K)	1.53
γ (mJ mol-at.$^{-1}$ K^{-2})	1.56
θ_D (K)	341
$\theta_{RM,6}$ (K)	21
$\Delta C_{el}/\gamma T_c$	1.42
λ_{ep}	0.42, 0.51[a]
$N(E_F)$ (states eV^{-1} f.u.$^{-1}$)[a]	5.2, 4.9
Δ_0/k_BT_c	1.71
Δ_0 (meV)	0.23
$\mu_0H_{c1}(0)$, $\mu_0H_{c2}(0)$, $\mu_0H_c(0)$ (Oe)	37, 800, 148
$\xi_{GL}(0)$ (nm)	64
$\lambda_{GL}(0)$ (nm)	245
κ	3.8

[a] For $\mu^* = 0.10$ and 0.15, respectively.

of the gap is the same as for the BCS theory. Although originally developed for strongly coupled superconductors, the α-model has also been applied to superconductors having weaker coupling than predicted by BCS, for example Zn [21]. Our data for $VAl_{10.1}$ is well described by the α-model using a single gap value of $\Delta_0/k_BT_c = 1.71$. This is slightly smaller than the BCS value of $\Delta_0/k_BT_c = 1.764$ and again points to weak-coupling superconductivity in $VAl_{10.1}$. From this value of Δ_0/k_BT_c and the transition temperature of $T_c = 1.53$ K we estimate a zero-Kelvin gap of $\Delta_0 = 0.23$ meV.

In summary, we have confirmed superconductivity and characterized normal- and superconducting-state physical parameters for the Einstein solid $VAl_{10.1}$. We show that $VAl_{10.1}$ is a BCS-type, weak-coupling superconductor. This contrasts with the β-pyrochlores AOs_2O_6 (A = Cs, Rb, K), where rattling of the alkali metal guests seems to mediate Cooper pairing [6]. In the pyrochlores the coupling becomes progressively stronger as guest size decreases, and rattling frequency decreases, from Cs^+ to Rb^+ to K^+. For strong coupling KOs_2O_6 the relevant rattling mode for superconductivity has the Einstein temperature $\theta_E \approx 60$ K [6]. For weak coupling $VAl_{10.1}$ the rattling frequency is much smaller, $\theta_E \approx 22$ K. However, the role of the Al guest rattling in the superconductivity is so far unclear. At present we know of only four members of the MV_2Al_{20} family, M = Al, Gd, Eu, and U [22–24], and only M = Al is known to superconduct. Based on the flexibility of the $Mg_3Cr_2Al_{18}$-type structure there are likely more possibilities for M. A study of MV_2Al_{20} compounds where the size of M is systematically changed will help us to understand the interplay between superconductivity and rattling in this family of Einstein solids.

Acknowledgments

The work at Los Alamos National Laboratory was supported in part by the Department of Energy's Laboratory Directed Research and Development Program. The work in Poland was supported by the National Science Centre (Poland) under Grant No. 2011/01/B/ST3/04482. TK acknowledges the European Commission for financial support in the frame of the 'Training and Mobility of Researchers' programme.

References

[1] Sales B C, Chakoumakos B C, Jin R, Thompson J and Mandrus D 2001 *Phys. Rev.* B **63** 245113
[2] Paschen S, Tran V H, Baenitz M, Carrillo-Cabrera W, Grin Yu and Steglich F 2002 *Phys. Rev.* B **65** 134435
[3] Goto T, Nemoto Y, Yamaguchi T, Akatsu M, Yanagisawa T, Suzuki O and Kitazawa H 2004 *Phys. Rev.* B **70** 184126
[4] Beekman M, Schnelle W, Borrmann H, Baitinger M, Grin Yu and Nolas G S 2008 *Phys. Rev. Lett.* **104** 018301
[5] Sales B C, Chakoumakos B C and Mandrus D 2000 *Phys. Rev.* B **61** 2475
[6] Nagao Y, Yamaura J I, Ogusu H, Okamoto Y and Hiroi Z 2009 *J. Phys. Soc. Japan* **78** 064702
[7] Teyssier J, Lortz R, Petrovic A, van der Marel D, Filippov V and Shitsevalova N 2008 *Phys. Rev.* B **78** 134504
[8] Christensen M, Abrahamsen A B, Christensen N B, Juranyi F, Andersen N H, Lefmann K, Andreasson J, Bahl C R H and Iversen B B 2008 *Nature Mater.* **7** 811
[9] Yoshida M, Arai K, Kaido R, Takigawa M, Yonezawa S, Muraoka Y and Hiroi Z 2007 *Phys. Rev. Lett.* **98** 197002
[10] Caplin A D, Grüner G and Dunlop J B 1973 *Phys. Rev. Lett.* **30** 1138
[11] Legg G J and Lanchester P C 1973 *J. Phys. F: Met. Phys.* **8** 2125
[12] Claeson T and Ivarsson J 1977 *Commun. Phys.* **2** 53
[13] Safarik D J, Klimczuk T, Llobet A, Byler D D, Lashley J C, O'Brien J R and Dilley N R 2012 *Phys. Rev.* B **85** 014103
[14] Brown P J 1957 *Acta Crystallogr.* **10** 133
[15] Ray A E and Smith J F 1957 *Acta Crystallogr.* **10** 604
[16] Klimczuk T and Cava R J 2004 *Phys. Rev.* B **70** 212514
[17] Cohen R W and Abele B 1968 *Phys. Rev.* **168** 444
[18] Werthamer N R, Helfand E and Hohenberg P C 1966 *Phys. Rev.* **147** 295
[19] Mühlschlegel B 1959 *Z. Phys.* **155** 313
[20] McMillan W L 1968 *Phys. Rev.* **167** 331
[21] Padamsee H, Neighbor J E and Shiffman C A 1973 *J. Low Temp. Phys.* **12** 387
[22] Verbovytsky Yu, Latka K and Tomala K 2007 *J. Alloys Compounds* **442** 334
[23] Chi J, Li Y, Gou W, Goruganti V, Rathnayaka K D D and Ross J H Jr 2008 *Phys.* B **403** 1426
[24] Halevy I, Sterer E, Aizenshtein M, Kimmel G, Regev D, Yahel E, Pereira L C J and Goncalves A P 2001 *J. Alloys Compounds* **319** 19